

Label-free Estimation of Sarcomere Orientation from Brightfield Microscopy Images of Induced Pluripotent Stem Cell Derived Cardiomyocyte Nuclei

Antti Ahola¹, Birhanu Belay¹, Carolina Wählby², Jari Hyttinen¹

¹Faculty of Medicine and Health Technology, Tampere University, Tampere, Finland

²Dept. IT and SciLifeLab, Uppsala University, Uppsala, Sweden

Abstract

Human induced pluripotent stem cell derived cardiomyocytes (hiPSC-CMs) provide a platform for studying disease models and physiological conditions. Sarcomere structure orientation can be used to determine hiPSC-CM culture maturity. However, novel methods are needed for assessing their structure and cellular function. Brightfield microscopy enables continuous label-free measurement of cell cultures in vitro. Here, we propose evaluating sarcomere organization from the morphology and orientation of nuclei in brightfield images.

We used publicly available image dataset consisting of brightfield complemented with stained nuclei and α -actinin. We trained a U-Net-based network for segmenting nuclei from brightfield images (IOU of 0.72) and extracted the orientation and aspect ratio of the predicted and stained nuclei. We quantified myofibrillar orientation from α -actinin and determined how it related to nuclei. The analysis revealed correlation between elongated nuclei and the orientation of the surrounding myofibrils.

Our results indicate that brightfield data alone can provide estimates of cellular structures without staining. This provides the means to assess structure and maturity from repeated measurements of unstained cells, enabling high-throughput quantification of the in-vitro cardiomyocyte mechanobiology.

1. Introduction

Human induced pluripotent stem cell (hiPSC) derived cardiomyocytes (CMs) have been used for cellular physiology-, cardiac disease- and drug studies *in vitro*. Their electrophysiological and biomechanical phenotype is, however, immature and their sarcomere structure not well organized. This structure is typically studied using immunofluorescent staining or genetic modification of cell lines, making continuous evaluation of CM culture difficult. Further, staining could also alter the physiological conditions of the cells. Development of label-free quantitative methods capable of providing this

information would enable continuous monitoring of CM maturation. The nucleus morphology and sarcomere orientation could be used here as physical properties for quantifying CM maturity.

U-Net-based networks [1] have been widely used in numerous applications in biomedical image analysis. Here, we implemented a residual [2] attention [3] U-Net and trained it using DAPI- and Nuclear Violet LCS1-stained nuclei images for segmenting CM nuclei from brightfield microscopy images. We quantified the orientation of sarcomeres around the nuclei and our results revealed that the sarcomere orientation aligned with the orientation of elongated nuclei, similarly observed in previous studies with animal models [4]. This work, combining image processing and machine learning, provides label-free methods that can be used in CM culture studies to monitor the maturation of hiPSC-CMs and contributes to development of novel differentiation techniques. In addition, the method could be applied to study models of genetic cardiac disease such as myopathies, which affect the sarcomere structure and nucleus.

2. Materials and Methods

2.1. Cardiomyocyte dataset

The image data used in the study was obtained from a dataset published by Gerbin et al. [5], consisting large field-of-view (FOV) images of hiPSC-CMs from a ACTN2-mEGFP hiPSC line. From the dataset, we used brightfield, DAPI- and Nuclear Violet LCS1-stained nuclei and mEGFP-tagged alpha-actinin-2 images. We divided the FOV image data to train and test sets, with 402 and 820 images, respectively. Due to graphics processing unit memory limitations, the 1776x1736 px FOV images (pixel size of 0.124 μm x 0.124 μm) were downsampled by 50 %, and 256x256 px patches were generated, resulting in 3295 training and 7353 test set images.

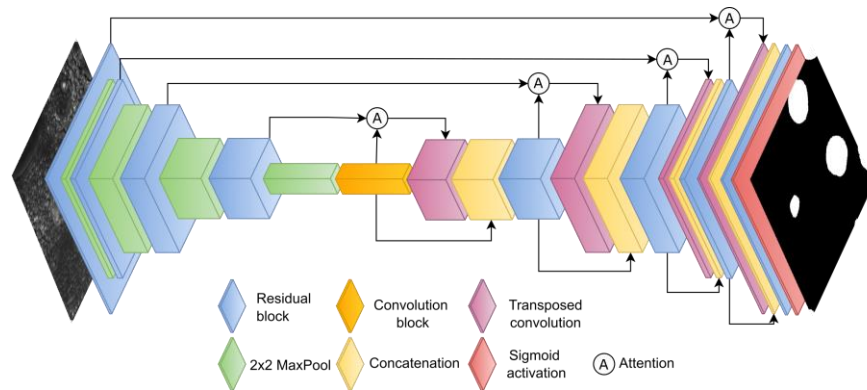


Figure 1: The network architecture of the implemented residual attention U-Net for segmenting nuclei (right side) from brightfield microscopy images (left side).

2.2. Network architecture

We implemented a residual attention U-Net for segmenting CM nuclei from the 256x256 px brightfield grayscale image patches in Python, using Keras. The network consists of U-Net architecture [1] – an encoder and a decoder, with skip connections between them. The architecture is illustrated in Figure 1. The network starts with 14 filters, doubling for each encoding layer and halving for each decoding layer.

Each residual block consists of 3x3 convolution, ReLU activation, 3x3 convolution, addition of a residual connection from the input [2], and a final ReLU activation. The attention takes the skip connection and the output of the layer below as a gating signal, described in detail in the original publication [3]. The role of the residual connections in encoder and decoder blocks is to address the vanishing and exploding gradient problem, helping the training of the network. The role of the attention blocks in decoding layers is to improve the focusing of the network on the desired regions.

2.3. Segmentation training

The network was trained to predict nuclei segmentation from brightfield images. For this purpose, images of DAPI- and LCS1-stained nuclei were first binarized using minimum threshold method to generate 256x256 masks, for both training and test sets. Binary cross-entropy was used as a loss function. The network was then trained with a batch size of 16 until the loss did not improve, in 7 epochs. We used the model to predict the segmentation of nuclei in the test set. The accuracy of the achieved segmentation was determined by comparing the predicted segmentation with the known segmentation (from the thresholded stained image) in the test set using the intersection over union (IOU) metric.

For individual nuclei segmentations, we discarded

segmentations below 5000 and above 13000 pixels to remove overlapping nuclei and nuclei that were only partially visible.

2.4. Orientation analysis

To study the organization of sarcomere structure and elongated nuclei, we quantified the shape of the nuclei segmentations by ellipse fitting for stained and predicted nuclei. Around each nucleus, we fitted an ellipse and determined its axes aspect ratio (major/minor axes). Further, we determined its rotation and estimated the ellipse fit by calculating the ratio between the ellipse and nucleus area.

The underlying sarcomere structure orientation of each segmented nucleus was quantified using CytoSpectre software [6], which uses spectral analysis to determine orientation and wavelength distribution in images. Here the detail component, expressing the orientation distribution of the z-disc striated myofibers in the image, was determined.

The rotations of the ellipses fitted to the predicted and stained nuclei were compared with the orientation of their underlying sarcomere structures – for stained nuclei, predicted nuclei, false positives, and false negatives.

We removed nuclei with area per ellipse area above 1.06 due to poor ellipse fit. For statistical analysis, we selected a random sample of maximum 300 nuclei and calculated Pearson correlation and coefficient of determination between the orientations for aspect ratios of >1 , >1.25 and >1.5 .

3. Results

3.1. Prediction of nuclei segmentation

We evaluated the U-Net-based segmentation model by calculating IOU for the 256x256 patches. The mean IOU was 0.72 with a standard deviation of 0.27, and 49 % of images reached $\text{IOU} > 0.8$. Representative predictions with different IOU are shown in Figure 2. The figure shows predictions with high IOU values that accurately approximate the nuclei locations and shapes. The middle prediction, with an IOU near the mean, shows inaccuracies in the nuclei boundaries and image borders, while still pertaining the shape of the nuclei. A below-mean IOU prediction shows the network missing a nucleus.

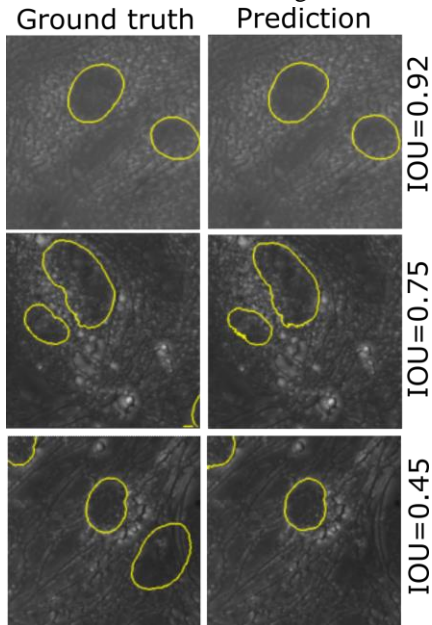


Figure 2: Ground truths and predictions of different accuracies: top image shows an accurate prediction ($\text{IOU}=0.92$), middle a good prediction with inaccuracies on the nuclei and image boundaries ($\text{IOU}=0.75$), and the bottom a prediction with a missing nucleus ($\text{IOU}=0.45$).

For the orientation analysis of the nucleus and the underlying sarcomere structure, after applying the exclusion criteria listed in 2.4, we obtained 7819 stained nuclei and 6180 predicted nuclei for the analysis. Out of these, we determined 895 of the predicted nuclei to be false positives and 2648 of the stained nuclei to be false negatives – resulting in precision of 0.856 and recall of 0.666.

3.2. Nuclei and sarcomere co-orientation

We studied the co-orientation of nuclei and their underlying sarcomere structure. Based on the nucleus segmentation, we partitioned the nuclei into groups with different aspect ratios, as shown in Table 1. The number of elongated network-predicted nuclei was low: only 309 (5% of all predicted nuclei) as opposed to 1134 (15% of all stained nuclei).

Table 1. The number of nuclei for different aspect ratios in stained and predicted sets, including false negatives and positives

Aspect ratio	<1.1	1.1-1.2	1.2-1.3	1.3-1.4	1.4-1.5	>1.5
Stained	652	1519	1910	1604	1000	1134
Predicted	1004	1899	1608	907	453	309
False neg.	160	427	576	557	369	559
False pos.	123	221	204	136	91	120

Further, we plotted a histogram in Figure 3 illustrating the distribution of co-oriented stained and predicted nuclei and sarcomeres, with respect to nucleus aspect ratio. The histogram shows that nuclei with an aspect ratio of below 1.10 are angle-wise randomly distributed, with higher aspect ratios having more peaked distributions. The network-generated nuclei have less nuclei with very high aspect ratio than the stained nuclei, making the histogram wider.

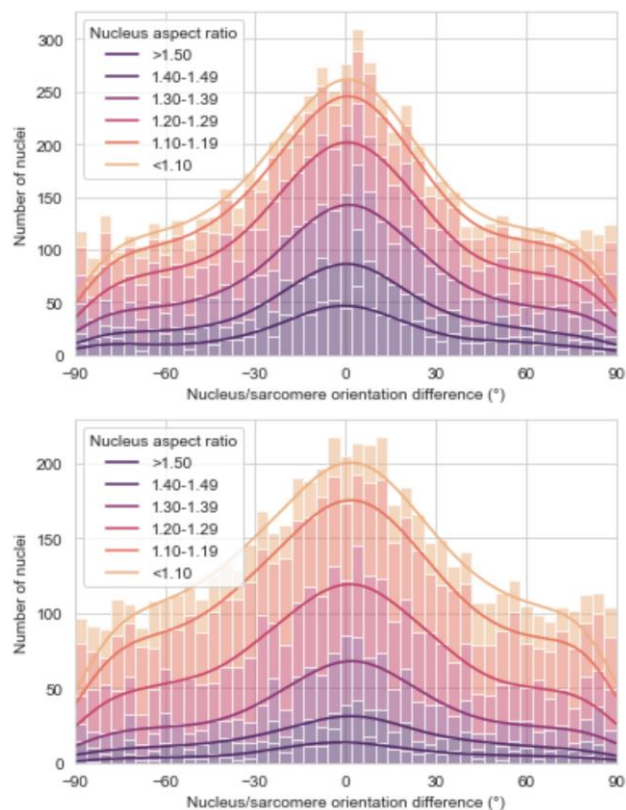


Figure 3: Histograms showing the co-orientation of stained (above) and predicted (below) nuclei and sarcomere structure as a function of nucleus aspect ratio.

4. Discussion

Here, we implemented residual attention U-Net

architecture and trained it to segment hiPSC-CM nuclei from brightfield microscopy images. The morphology of the predicted and stained nuclei was then parametrized using ellipse fitting. Their underlying sarcomere structure orientation was quantified and compared with the nuclei orientation.

Our results indicate that U-Net based prediction of CM nuclei from brightfield images is feasible. It can be used to estimate the location of nuclei in a monolayer and obtain morphological information without the need of staining. The number of false negatives was high, resulting in modest specificity. Training on non-scaled images and image pre-processing, such as log-transform, could be beneficial for revealing textures relevant for the network and improving the specificity. The precision of the network was higher, and it could further be improved by reducing false positives during post-processing, such as by filtering out shapes that do not resemble nuclei.

The orientation analysis revealed that the shape of cell nuclei (measured as aspect ratio) correlates with their associated sarcomere structure. The co-orientation histograms showed the predicted nuclei to be more round-shaped than the stained nuclei. The number of false negatives in elongated nuclei could be improved by balancing the training dataset regarding the aspect ratio. Our results reveal that predicted nuclei shapes can be used to estimate the orientation of sarcomere structures without staining or using genetically modified cell lines.

Moreover, our developed nuclei segmentation and orientation analysis methods based on brightfield microscopy images enable analysis of cellular morphology and orientation. Further, this analysis can be combined with our previously developed quantification of contractility using brightfield video-based measurements [7] to provide more detailed estimates of the sarcomere structure and biomechanics.

This analysis of CM nuclei could be applied in label-free monitoring of CM maturation in culture. It does not require fixing the cells for staining, avoiding the potential of perturbing the physiological condition of the cells. Furthermore, it can be used to augment drug studies, where high-throughput analysis methods are advantageous. This model could be used in studies involving genetic cardiac disease specific CM models affecting the sarcomere and nuclear structure, such as cardiomyopathies.

5. Conclusions

We found that residual attention U-Net trained using DAPI- and LCS1-stained nuclei images can accurately predict CM nuclei shape and orientation from brightfield images. Further, we revealed that the nuclei orientation has an axes aspect ratio -dependent correlation with their underlying sarcomere structure orientation. Together, these findings enable estimation of sarcomere structure orientation from nuclei imaged by brightfield microscopy

without staining. This morphological and orientation analysis can be applied to understand CM biomechanics, for continuous assessment of CM maturation, in high throughput applications such as drug screening, and in genetic cardiac disease studies.

Acknowledgments

This study was funded by a personal grant from Finnish Cultural Foundation Pirkanmaa regional fund. We would like to acknowledge Nicolas Pielawski for valuable input during model building.

References

- [1] O. Ronneberger, P. Fischer, and T. Brox, "U-Net: Convolutional Networks for Biomedical Image Segmentation BT - Medical Image Computing and Computer-Assisted Intervention - MICCAI 2015," 2015, pp. 234–241.
- [2] Z. Zhang, Q. Liu, and Y. Wang, "Road Extraction by Deep Residual U-Net," *IEEE Geosci. Remote Sens. Lett.*, vol. 15, pp. 749–753, 2018.
- [3] O. Oktay *et al.*, "Attention U-Net: Learning Where to Look for the Pancreas." arXiv, 2018, doi: 10.48550/ARXIV.1804.03999.
- [4] M.-A. P. Bray, W. J. Adams, N. A. Geisse, A. W. Feinberg, S. P. Sheehy, and K. K. Parker, "Nuclear morphology and deformation in engineered cardiac myocytes and tissues.," *Biomaterials*, vol. 31, no. 19, pp. 5143–5150, Jul. 2010, doi: 10.1016/j.biomaterials.2010.03.028.
- [5] K. A. Gerbin *et al.*, "Cell states beyond transcriptomics: Integrating structural organization and gene expression in hiPSC-derived cardiomyocytes," *Cell Syst.*, vol. 12, no. 6, pp. 670-687.e10, 2021, doi: <https://doi.org/10.1016/j.cels.2021.05.001>.
- [6] K. Kartasalo *et al.*, "CytoSpectre: a tool for spectral analysis of oriented structures on cellular and subcellular levels," *BMC Bioinformatics*, vol. 16, no. 1, p. 344, 2015, doi: 10.1186/s12859-015-0782-y.
- [7] A. Ahola, A. L. Kiviaho, K. Larsson, M. Honkanen, K. Aalto-Setälä, and J. Hyttinen, "Video image-based analysis of single human induced pluripotent stem cell derived cardiomyocyte beating dynamics using digital image correlation.," *Biomed. Eng. Online*, vol. 13, no. 1, p. 39, 2014, doi: 10.1186/1475-925X-13-39.

Address for correspondence:

Antti Ahola
Tampere University
Korkeakoulunkatu 7, 33720, Tampere, Finland
antti.ahola@tuni.fi